Research in International Business and Finance 75 (2025) 102727

Contents lists available at ScienceDirect

Research in International Business and Finance

journal homepage: www.elsevier.com/locate/ribaf

Is gold in the process of a bubble formation? New evidence from the ex-post global financial crisis period

Klaus Grobys [1]

Innovation and Entrepreneurship (InnoLab), University of Vaasa, Wolffintie 34, Vaasa 65200, Finland
Finance Research Group, School of Accounting and Finance, University of Vaasa, Wolffintie 34, Vaasa 65200, Finland

ARTICLE INFO

JEL Classification:
C22
G12
G13
G14
O10

Keywords:
Bubble
Gold
Finite-time singularity
Log-periodic power laws
Singularity

ABSTRACT

In the prices of financial assets, super-exponential growth is not sustainable and will eventually result in what physicists term a "finite-time singularity," suggesting an abrupt transition into a new regime—which often manifests itself in a crash. The financial literature on gold has documented that the dynamics constituting the supply-and-demand relationship in the market for gold has undergone substantial changes since the early 2000s. In particular, the global financial crisis might have had an unprecedented effect on the demand for gold as a financial asset. This is the first paper exploring whether gold is in the process of a bubble formation that started in the ex-post financial crisis period. Calibrating the log-periodic power law (LPPLS) model to the log-prices of gold futures using daily data covering the period December 2015—June 2024, this study finds strong evidence for a bubble formation predicted to last until 2029. Various robustness checks provide further evidence that the LPPLS model is a remarkable tool for predicting bubble formations in the market for gold.

1. Introduction

Gold is often regarded as a "safe haven" because of its lack of correlation with returns on stock. In this regard, Baur and McDermott (2010) concluded that gold acts as a stabilizing force for the financial system by reducing losses in the face of extreme negative market shocks. The authors found that gold served as a strong safe haven for most developed markets during the peak of the 2008–2009 global financial crisis (GFC). However, O'Connor et al., 2015 highlighted that the creation of the first gold Exchange Traded Fund (ETF)—the Gold Bullion Securities ETF backed by the World Gold Council—which took place in 2003, was the start of a major change. The authors stressed the following:

> Whether gold's ability to act as a safe haven has been reduced because it is now being held more and more as a speculative investment through vehicles such as ETFs will require more time and data. (O'Connor et al., 2015, p. 196)

Baur (2013) concluded that the launch of ETFs led to a structural shift in the drivers leading to a demand for gold because it generated a new source of investment demand for gold, enabling smaller investors to purchase gold in a simple way. O'Connor et al., (2015) argued that this issue seems to have been—at least partially—responsible for the consistent rise in gold prices in the ex-post GFC period. Notably, O'Connor et al., (2015) highlighted that, in the wake of the GFC, three structural changes have been observed in the market for gold:

E-mail address: klaus.grobys@uwasa.fi.

[1] The author is thankful to two anonymous reviewers for providing useful comments.

https://doi.org/10.1016/j.ribaf.2024.102727
Received 3 September 2024; Received in revised form 12 November 2024; Accepted 21 December 2024
Available online 24 December 2024

(a) The attraction of rising prices and increased concerns about the riskiness of other investments following the GFC resulted in an increased demand for gold in the Western world.
(b) In the wake of the GFC, central banks became net buyers of gold again in 2010 for the first time since the 1980s.
(c) The GFC marked a breaking point in the nature of gold spillovers, weakening it considerably, whereas that of other precious metals, such as platinum, increased.

In sum, the evidence has suggested that the ex-post GFC period has been characterized by substantial changes in the market for gold. Because of rising speculation through vehicles such as ETFs, the question arises as to whether the sharp rise in the prices for gold in the ex-post GFC period manifests as an ongoing bubble formation.

Hence, the present study attempts to answer the question of whether gold is in the process of an ongoing bubble formation. A typical manifestation of bubble formations is faster-than-exponential growth, which is, however, not sustainable and will eventually result in what physicists term a "finite-time singularity," that is, an abrupt transition into a new regime (Sornette, 2017).[2] Does the price evolution for gold exhibit bubble formation manifested in faster-than-exponential growth? The present study is the first to investigate whether the log-prices of gold—here measured in terms of the prices for gold futures—exhibit unsustainable, respectively, super-exponential growth in the ex-post GFC period.

To examine this issue, we search for a local minimum (i.e., trough) in the price process of gold futures in the ex-post GFC period and calibrate a log-periodic power law singularity (LPPLS) model using data ranging from the identified trough until the end of our sample (i.e., June 11, 2024). The rationale for using the LPPLS model is that it demonstrates outstanding performance in predicting bubble formations (e.g., Shu and Zhu, 2020; Wheatley et al., 2019; Zhou and Sornette, 2006, 2009). As pointed out in Wheatley et al. (2019), the LPPLS model is capable of addressing some universal features manifested in bubble formations: (a) It is capable of modeling price processes exhibiting transient faster-than-exponential growth (i.e., where the growth rate itself is growing)—resulting from positive feedback mechanisms such as herding, and (b) it accounts for accelerating log-periodic volatility fluctuations, which embody spirals of competing expectations of higher returns (bullish) and an impending crash (bearish). Notably, such log-periodic fluctuations are universal in complex systems (Sornette, 2017). To calibrate the LPPLS model, we use the three-step estimation approach recently proposed by Grobys (2023). To test whether the LPPLS signature is statistically significant, we employ augmented Dickey–Fuller (ADF) tests to assess whether the residuals of the optimized LPPLS model exhibit stationarity (Lin et al., 2014). Furthermore, we check the predictive power of the LPPLS model by expanding the data set, identifying three historical bubble formations: The first bubble formation is from January 16, 1970, until December 30, 1974, the second bubble formation is from August 30, 1976, until January 21, 1980, and the third bubble formation is from July 19, 1999, until August 22, 2011. When calibrating the LPPLS models to examine their capability of identifying historical bubble formations in the market for gold, we follow the common literature on LPPS models (e.g., Grobys, 2023; Sornette, 2017) and condition the data set so that the last year of observations before reaching each local peak is excluded. Again, we test for statistical significances of LPPLS signatures by implementing various ADF tests.

The present study contributes to the literature in several important ways. For example, O'Connor et al., 2015 provided an extensive review of the literature on exploring bubble formations in the prices for gold. The authors documented that the literature on this issue is inconclusive. Furthermore, O'Connor et al., 2015 highlighted that the vast majority of the literature has employed the convenience yield (CY) model, forward recursive ADF tests, or one of those approaches combined with a Markov switching model. Interestingly, Johansen and Sornette (1999) were the first to calibrate the LPPLS model using the log-prices of gold futures. The authors found evidence for an *anti*bubble in the log-prices of gold futures between 1980 and the late 1990s. However, no study has yet explored whether the prices of gold futures would manifest bubble behavior in the ex-post GFC period—a period in which the market for gold has undergone some substantial changes (O'Connor et al., 2015). Potential bubble formation—which is inevitably followed by some regime switch that could manifest in a collapse—could cause harm to investors wishing to diversify asset portfolio risk using gold futures. Moreover, the estimated global gold market capitalization exceeded USD 18 trillion in September 2024.[3] For comparison, a 15 % drop in the price for gold implies a loss that is greater than the overall market capitalization for cryptocurrencies.[4] Indeed, gold—considered a single asset—has the highest market capitalization across all asset classes. Therefore, by investigating whether gold is subject to potential ongoing bubble formation, the present study fills an important gap in the literature. In doing so, it adopts the LPPLS model, which demonstrated a remarkable level of reliability in detecting bubble formations (e.g., Shu and Zhu, 2020; Wheatley et al., 2019; Zhou and Sornette, 2006, 2009).

Next, taking a wider perspective, the current study adds to the literature on the potential arrival of finite-time singularities manifested in regime switches, specifically in the dynamics of socio-economic data. For example, in their pioneering work, Johansen and Sornette (2001) analyzed the potential arrival of finite-time singularities in the dynamics of the world population and some leading financial indices; the authors predicted the arrival of a spontaneous singularity around 2050, signaling an abrupt transition into a new regime. Sornette (2017) provided an extensive review of the literature exploring LPPLS signatures in equity markets. A recent study by Grobys (2023) used an expanded sample covering the January 1871 to November 2022 period and monthly data on

[2] For example, the stock market crash as of October 19, 1987, can be considered the archetype of such a finite-time singularity. Note that Sornette (2017) elaborates on various scenarios in which finite-time singularities could manifest themselves. The first and perhaps most intuitive potential scenario is a "collapse," the second possible scenario is a "transition to sustainability," and the third is "resuming accelerating growth" by overcoming fundamental barriers.

[3] See https://companiesmarketcap.com/gold/marketcap/#google_vignette, accessed on November 6, 2024.

[4] According to coinmarketcap.com, the total market capitalization for the market for cryptocurrencies is USD 2.46 trillion as of November 6, 2024.

S&P 500 data to re-examine whether the US equity market would exhibit an LPPLS signature. His results confirmed the findings of Johansen and Sornette (2001) and suggested the arrival of a regime switch in 2050. Another recent study in this stream of research was that of Grobys (2024) documenting that Bitcoin is subject to a log-lasting bubble formation. Grobys' (2024) calibrated LPPLS model suggested that Bitcoin will experience a finite-time singularity condition close to the year 2140. Whereas Johansen and Sornette (2001) and Grobys (2023; 2024) provided real out-of-sample forecasts, the vast majority of finance studies have been, according to Taleb, (2020), typically subject to "postdiction." As a result, the present study adds to the literature on out-of-sample predictions by investigating whether the market for gold futures exhibits an LPPLS signature that would suggest the arrival of a finite-time singularity after 2024. Additionally, to examine the reliability of the LPPLS model in predicting historical bubble formations in the market for gold, we calibrate our model to three historical gold bubble formations—that is, gold bubbles in the 1970s, 1980s, and early 2000s.

For the main analysis, we examine daily data on gold futures covering the ex-post GFC period from January 2, 2010, until June 11, 2024. We find that the prices for gold futures reached a local maximum on August 22, 2011, which is in line with the literature documenting that gold prices rose sharply in the wake of the GFC (O'Connor et al., 2015). We identify a local minimum (i.e., trough) in the prices for gold futures on December 2, 2015, with a closing price quoted at USD 1053.80. We calibrate the LPPLS model using Grobys' (2023) optimization procedure, using daily data on gold futures from December 2, 2015, to June 11, 2024. Strikingly, we find strong evidence for the arrival of a finite-time singularity occurring on October 6, 2029.

Astonishingly, the parameter capturing the angular log-frequency of oscillations during the formation of the bubble is estimated at $\omega \approx 15$ across all optimized models in the third stage of the optimization, hence suggesting a high level of parameter stability. Similarly, depending on the optimized model, the critical time varies between October 6, 2029, and November 5, 2029, which is a much narrower time interval than typically documented for LPPLS model predictions (e.g., Grobys, 2023). Further evidence suggests that virtually all parameters are normally distributed and highly statistically significant, which confirms Grobys' (2023) findings for calibrated LPPLS models using data on the S&P 500. Robustness checks show that the identified LPPLS signature is statistically significant because it fulfills the stationarity condition, as highlighted in Lin et al. (2014). Further evidence suggests that the LPPLS model can reliably predict bubble formations in the market for gold in the 1970s and 1980s. On the contrary, even though the LPPLS model suggests bubble formation in the early 2000s with a predicted critical time corresponding to July 21, 2007, the burst of the bubble failed to materialize. A possible explanation for this "false positive" could be that, as early signs of the housing market collapse started to manifest already in the year 2006, investors moved their assets to gold and, by doing this, pushed the prices for gold to even higher levels, as anticipated by the LPPLS model. Similar evidence is documented by Grobys (2023), who failed to predict the US stock market crash as October 2008 using the LPPLS model because of "exogenous factors" counteracting the endogenous dynamics modeled via the LPPLS methodology.

The present paper is organized as follows: The next section describes the data. The third section provides the methodology, and the fourth section documents the results. The fifth section discusses the main findings, and the last section concludes the paper.

2. Data

Data on gold futures (Gold Futures—Dec 24 (GCZ4)) are available from January 2, 2001, to June 11, 2024, and have been downloaded from investing.com.[5] The rationale for using data on futures is that futures are traded on exchanges and provide investors with more financial leverage, flexibility, and integrity than trading gold as an actual physical commodity.[6] The descriptive statistics for the daily log-returns on gold futures are reported in Table A.1 in the Appendix. The daily price evolution of gold futures is plotted in Fig. 1. A visual inspection of Fig. 1 shows that, following a local maximum on August 22, 2011—where the closing price for gold future was quoted at USD 1891.90—a local minimum can be found on December 2, 2015, where the closing price for gold future was quoted at USD 1053.80. Does the price evolution for gold futures in the ex-post December 2, 2015, period exhibit super-exponential growth? To explore this issue, we employ daily data from December 2, 2015, to June 11, 2024, to calibrate the LPPLS model.

3. Methodology

3.1. Implementing the LPPLS model using the daily log-prices of gold futures

A plain power law model for financial log-prices is given by the following:

$$\ln[p(t)] = A + B(t_c - t)^{\beta}, \tag{1}$$

where $\ln[p(t)]$ denotes the logarithm of gold futures at time t, t_c is the critical time, A is the expected value of gold futures when approaching t_c, B defines the exposure to faster-than-exponential growth, and β is the power law exponent controlling faster-than-exponential price growth (Sornette, 2017). The critical time t_c indicates the end of the accelerating oscillations, which results in a finite-time singularity manifested in a regime change (Zhang et al., 2016). According to Sornette (2017), the following constraints need to be imposed:

[5] Investing.com obtained data from Commodity Exchange ICE.

[6] Another study that used price data on gold futures was Johansen and Sornette (1999). In what follows, gold prices and prices for gold futures are used interchangeably throughout.

Fig. 1. The price evolution of gold futures during the 2001—2024 period.

$A > 0$,

$B < 0$,

$0.1 \leq \beta \leq 0.9$.

In addition, the simple power law model of Eq. (1) needs to be extended by accounting for periodic oscillations:

$$\ln[p(t)] = A + B(t_c - t)^{\beta}[1 + C\cos(\omega \ln(t_c - t) + \phi)], \tag{2}$$

where C denotes the exposure of the log-periodic oscillations around the power law singular growth, ω denotes the angular log-frequency of oscillations during the formation of the bubble, ϕ is the phase parameter, and all other notations are as previously defined. Note that Sornette (2017) stressed that parameter ϕ cannot be meaningfully restricted. Following earlier research, we require $|C| < 1$ and impose the constraint $5 \leq \omega \leq 15$ (Grobys, 2023). To estimate the parameter vector $\mathbf{\Phi} = (A, B, t_c, \beta, C, \phi)$ given by Eq. (2), we employ Grobys' (2023) recently proposed approach to calibrate the LPPLS model; that is, first, we set $B = -1$, $t_c = T + 1$, and $A = \ln[p(T)]$, where $p(T)$ denotes the logarithm of gold futures at time t. Then, we optimize four models by using Eq. (1), where only the initial values for β vary: $\beta \in \{0.20, 0.40, 0.60, 0.80\}$. To find the optimal solutions for a given model specification, we use the nonlinear solver provided from MS Excel. Because we use daily data on gold futures and 2147 daily observations, $t_c = T + 1 = 5.9011$.

In line with earlier research, we select the model generating the minimum sum of squared residuals (SSR) with the corresponding optimal parameter vector $\mathbf{\Phi}_1^* = (A^*, B^*, t_c^*, \beta^*)$. The numerical values of $\mathbf{\Phi}_1^*$ are then used as the starting value in the next step of the optimization procedure. That is, employing $\mathbf{\Phi}_1^*$ as initial values for model 2 in Eq. (2) while setting $C = \phi = 0$, model 2 is then optimized for varying values ω: $\omega \in \{5, 6, \ldots, 14, 15\}$. To optimize model 2, the following constraints are accounted for:

$t_c \geq T + 1$,

$0.1 \leq \beta \leq 0.9$,

$5 \leq \omega \leq 15$.

The parameter vector $\mathbf{\Phi}_2^* = (\mathbf{\Phi}_1^*, C, \omega, \phi)$ is used for the numerical starting values in the optimization, where $\mathbf{\Phi}_1^* = (A^*, B^*, t_c^*, \beta^*)$ and $C = \phi = 0$, for each given $\omega \in \{5, 6, \ldots, 14, 15\}$. As in the first step, model 2 in Eq. (2) is optimized by employing Microsoft Excel's nonlinear solver. As a result, 11 optimized parameter vectors $\mathbf{\Phi}_{2j}^{**} = \left(A_j^{**}, B_j^{**}, t_{c,j}^{**}, \beta_j^{**}, C_j^{**}, \omega_j^{**}, \phi_j^{**}\right)$ are obtained with $j = 1, \ldots, 11$. The optimal model is selected with respect to the minimum SSR generated (Grobys, 2023).

3.2. Robustness checks

To check the robustness of the LPPLS signature, we test whether the residual process exhibits stationarity (Lin et al., 2014) by means of the standard ADF test (Grobys, 2023). In line with earlier studies, calibrations with the 99 % confidence level of stationarity of the residuals derived from the optimal parametrization $\mathbf{\Phi}_{2j}^{**}$ are considered statistically significant (Jiang et al., 2010). The ADF test requires the implementation of the following regression model:

$$\Delta e_t = \delta_0 + \delta_1 t + \delta_2 e_{t-1} + \gamma_1 \Delta e_{t-1} + \ldots + \gamma_p \Delta e_{t-p} + \epsilon_t, \tag{3}$$

where $e_t = p_t - m_t$ is the difference between the log-prices of gold futures and the calibrated optimal model using the parameter vector $\mathbf{\Phi}_{2,j}^{**}$ derived from using the corresponding ω minimizing SSR, t denotes a time trend, and ϵ_t is assumed to be an identically and independently distributed (IID) error term. From Eq. (3), it is evident that $\delta_0 = \delta_1 = 0$ defines a model specification with no deterministic terms, whereas $\delta_1 = 0$ defines a model with a constant term only. The parameters $\gamma_1,\ldots,\ \gamma_p$ measure exposure to the lagged terms $\Delta e_{t-1},\ldots,\ \Delta e_{t-p}$. Furthermore, the parametrization $\delta_0 = \delta_1 = 0$ defines a random walk as the null model, while the parametrization $\delta_1 = 0$ defines a random walk with a drift as the null model. Following earlier studies, the optimal lag-order p is selected in line with the Schwarz criterion (Grobys, 2023).

4. Results

4.1. Main results

We employ daily data from December 2, 2015, to June 11, 2024, to calibrate the models. Panel A of Table 1 reports the starting values for each simple power law model specification from using Eq. (1), and Panel B of Table 1 reports the optimized parameters. It becomes evident that the parameters $A = 7.7509$, $B = -1$, $\overline{\beta} = 0.20$, and $t_c = 5.9011$ produce the minimum SSR corresponding to 1366.65. Optimizing the model with this parametrization using the constraints $A > 0, B < 0, 0.10 \leq \beta$, and $\beta \leq 0.90$ gives us the model $\mathbf{\Phi}_1^* = \left(A^*,\ B^*,\ t_c^*,\ \beta^*\right) = (10.2959,\ -1.4338,\ 12.0423,\ 0.3274)$. The parameter vector $\mathbf{\Phi}_1^*$ is then employed in the next stage of optimization.

Next, we use $\mathbf{\Phi}_1^* = \left(A^*,\ B^*,\ t_c^*,\ \beta^*\right)$ as starting values for the next step of the optimization using $\mathbf{\Phi}_2^* = \left(\mathbf{\Phi}_1^*, C, \omega,\ \phi\right)$ with $C = \phi = 0$ as the starting values. Using these numerical values, we optimize model 2 for varying values of ω, that is, $\omega \in \{5,\ 6, \ldots, 14,\ 15\}$. We estimate the optimal values for the parameter vector $\mathbf{\Phi}_2^{**}$ using Microsoft Excel's nonlinear solver. Panel A of Table 2 reports the numerical starting values for the parameters used for the optimization procedures, whereas Panel B of Table 2 reports the optimized parameter values, along with the SSR. From Panel B of Table 2, it is evident that optimal parameterization for model 2—producing the least SSR (e.g., $SSR = 6.0080$)—is given by $A^{**} = 9.5698$, $B^{**} = -0.9368$, $t_c^{**} = 11.2183$, $\beta^{**} = 0.4085$, $C^{**} = 0.0379$, $\omega^{**} = 15.0000$, and $\phi^{**} = -14.7420$. This means that the optimal model 2 suggests that a finite-time singularity occurs at $t_c^{**} = 11.2183$, which corresponds to 5.3187 years (e.g., 1936 days) in the future. Because our sample ends at time $T = 5.8984$, the model estimates a finite-time singularity to arrive on October 6, 2029.

It is interesting to note that, regardless of optimized model 2, $\omega^{**} \approx 15$. Panel B of Table 2 also shows that the estimated log-price of gold futures at the critical time is surprisingly consistent across the optimized models and varies between $A^{**} = 9.5698$ and $A^{**} = 10.7060$. The same can be observed for t_c^{**}, which varies between $t_c^{**} = 11.2183$ (e.g., October 6, 2029) and $t_c^{**} = 11.2993$ (November 5, 2029). The descriptive statistics for the estimated parameters are reported in Table 3. From Table 3, it becomes evident that virtually all parameters are normally distributed and highly statistically significant.

Next, Fig. 2 plots the optimized model 2, which is denoted as Model* , for the in-sample time window (e.g., December 2, 2015, to June 11, 2024) along with the natural logarithm of the prices for gold futures, $p_t = \ln[P(t)]$.[7] Fig. 3 complements Fig. 2 by plotting the optimized model 2, which is denoted as Model* , for the in-sample time window and the out-of-sample time window. We can see from Fig. 3 that the optimal model suggests the arrival of finite-time singularity on October 6, 2029. Furthermore, the difference between the actual log-prices for gold futures and predicted log-price by means of the LPPLS model is defined as $e_t = p_t - m_t$, which is plotted in Fig. 4. Whereas visual inspections of Figs. 2 and 3 show that the optimized model 2 could offer a proper description for the evolution of log-prices for gold futures, Fig. 4 shows that the residual process exhibits stationarity.

However, to explicitly test for stationarity, we employ the ADF test. The results are reported in Table 4. Strikingly, from Table 4, it becomes evident that, regardless of the regression model, the $\widehat{\lambda} \approx -4.79$. Because the critical value for the 1 % level range—depending on the model specification—is between −2.56 and −3.96, we conclude that the random walk hypothesis is clearly rejected by a substantial margin. This result provides strong evidence that the ascertained LPPLS signature is indeed statistically significant (Lin et al., 2014).

4.2. Additional robustness checks: How did the LPPLS model perform in predicting historical gold bubbles?

We now explore whether the LPPLS model has predictive power for the bubbles that occurred in the past because making a specific prediction—as proposed in the main analysis—without providing further evidence supporting the predictive power of the LPPLS model could seem overly confident. To address this issue, data on gold are obtained from the Independent Precious Metals Authority via the webpage lbma.org.uk. This webpage provides daily price quotations of gold from January 2, 1968, onwards. Hence, for the robustness check, we retrieve daily data on gold covering the period January 2, 1968, until September 30, 2014. Fig. 5 shows the evolution of log-prices for gold during the sample from January 2, 1968, to September 30, 2014, comprising 11,770 daily observations. We identify three episodes of bubble formations: The first trough-to-peak period is from January 16, 1970, to December 30, 1974, with corresponding price quotations of USD 34.78 and USD 197.50. The second trough-to-peak period is from August 30, 1976, to January 21, 1980, with corresponding price quotations of USD 102.80 and USD 834.00, whereas the third trough-to-peak period is from July

[7] Note that Figure A.1 in the Appendix shows the prediction of the optimal model until the arrival of the finite-time singularity on October 6, 2029.

Table 1
Calibrating the power-law model for logarithmic prices of gold futures using the 2015—2024 sample.

Panel A. Initial parameter values for model 1.					
Specification	A	B	$\overline{\beta}$	$t_c = T + 1$	SSR
1	7.7509	−1	0.2	5.9011	1366.6500
2	7.7509	−1	0.4	5.9011	2544.9950
3	7.7509	−1	0.6	5.9011	4964.1100
4	7.7509	−1	0.8	5.9011	9727.8200
Panel B. Optimized parameter values for model 1.					
Specification	A^*	B^*	β^*	t_c^*	SSR
1	**10.2959**	**−1.4338**	**0.3274**	**12.0423**	**12.8287**
2	8.4127	−0.4695	0.5056	8.0514	13.1089
3	8.3597	−0.4640	0.5017	7.7890	13.1314
4	8.2519	−0.3596	0.5806	7.8993	12.9662

This table reports the estimated parameter for the plain log-period power-law singularity model. The estimation procedure is detailed in Section 3. Whereas Panel A of Table 1 reports the sum of squared residuals for several initial model specifications, Panel B of Table 1 reports the estimated parameter vector $\mathbf{\Phi}_1^* = (A^*, \quad B^*, \quad t_c^*, \quad \beta^*)$ under the constraints $t_c \geq T + 1$, and $0.1 \leq \beta \leq 0.9$. The sample period is from December 2, 2015 to June 11, 2024 comprising 2147 daily observations. **Bold** figures indicate the model exhibiting the minimum sum of squared residuals (SSR).

19, 1999, to August 22, 2011, with corresponding price quotations of USD 253.90 and USD 1891.90.

4.2.1. Performance of the LPPLS model to predict gold bubble formation in the 1970s

First, we explore whether the LPPLS model could detect and predict the bubble formation in gold prices in the 1970s. To do so, we use the sample from January 16, 1970, to December 31, 1973, which comprises 1005 daily observations as the in-sample period, to calibrate the LPPLS model. Because we exclude the observations from January 1, 1974, to December 30, 1974, this setup provides us with an out-of-sample prediction for t_c^{**}. In this regard, Sornette pointed out that "[a]pproximately a year before the crash, the fit begins to lock in on the date of the crash with increasing precision" (2017, p. 330). Note that the literature investigating the predictive power of the LPPLS model has typically examined model calibrations that exclude the last year of observations. Table 5 reports the results derived from the model specifications using Eq. (1), whereas Table 6 reports the results derived from the optimized LPPLS model specifications using Eq. (2). From Table 6, we observe that the optimal model 2 specification predicts $t_c^{**} = 5.2213$, which corresponds to March 6, 1975. Because the actual peak of the bubble was reached on December 30, 1974, the LPPLS model predicts the crash 47 days too late. Fig. 6 visualizes the time series evolution of the optimal LPPLS model along with the log-prices for gold covering a sample from January 16, 1970, until August 30, 1976, whereas Figure A.1 shows the evolution of the residuals derived from the optimal LPPLS model specification covering the in-sample period (viz., January 16, 1970, to December 31, 1973). In Table A.2. in the Appendix, the results from ADF tests are reported. We observe from Table A.2 that the test statistic derived from a test regression accounting for no deterministic terms suggests that the residuals plotted in Figure A.1 are stationary. Because unreported results suggest that neither the intercept in the ADF model specification accounting for an intercept nor the intercept or trend term in the ADF model specification accounting for intercept and trend term are statistically significant, the optimized LPPLS model indeed produces stationary residuals on a 1 % significance level, as indicated by the ADF model specification with no deterministic terms. Overall, the results suggest that the LPPLS model is indeed capable of (a) detecting bubble formation in the 1970s, as indicated by the statistically significant LPPLS signature and (b) predicting the critical time incorporating a regime switch with a relatively high reliability.

4.2.2. Performance of the LPPLS model to predict the gold bubble formation in the 1980s

Next, we investigate whether the LPPLS model could have detected the bubble formation in gold prices in the 1980s. To do so, we use the sample from August 30, 1976, to January 21, 1979, which comprises 622 daily observations as the in-sample period, to calibrate the LPPLS model. Again, we exclude the last year of observations. Table 7 reports the results derived from the model specifications using Eq. (1), whereas Table 8 reports the results derived from the optimized LPPLS model specifications using Eq. (2). From Table 8, we observe that the optimal model 2 specification predicts $t_c^{**} = 5.8515$, which corresponds to November 19, 1979. Because the actual peak of the bubble was reached on January 21, 1980, the LPPLS model predicts the crash 63 days too early. Fig. 7 visualizes the time series evolution of the optimal LPPLS model along with the log-prices for gold covering a sample from August 30, 1976, to December 31, 1980, whereas Figure A.2 shows the evolution of the residuals derived from the optimal LPPLS model specification covering the in-sample period (i.e., August 30, 1976, to January 21, 1979). In Table A.3 in the Appendix, the results from the ADF tests are reported. We observe from Table A.3 that various ADF test statistics suggest that the residuals plotted in Figure A.2 are stationary. Hence, the optimized LPPLS model indeed produces stationary residuals at a 1 % significance level. Overall, the results suggest that the LPPLS model is also capable of (a) detecting bubble formation in the 1980s as indicated by the statistically significant LPPLS signature, and (b) predicting the critical time with a relatively high reliability.

4.2.3. Performance of the LPPLS model to predict gold bubble formation in the early 2000s

Finally, we investigate whether the LPPLS model could have been able to detect and predict bubble formation in gold prices in the early 2000s. To do so, we use the sample from July 19, 1999, to September 14, 2006, which comprises 1745 daily observations as the

Table 2
Optimizing the log-period power-law singularity model for logarithmic prices of gold futures using the 2015—2024 sample.

Panel A. Initial parameter values for model 2.											
Specification	1	2	3	4	5	6	7	8	9	10	11
A^*	10.2959	10.2959	10.2959	10.2959	10.2959	10.2959	10.2959	10.2959	10.2959	10.2959	10.2959
B^*	−1.4338	−1.4338	−1.4338	−1.4338	−1.4338	−1.4338	−1.4338	−1.4338	−1.4338	−1.4338	−1.4338
t_c^*	12.0423	12.0423	12.0423	12.0423	12.0423	12.0423	12.0423	12.0423	12.0423	12.0423	12.0423
β^*	0.3274	0.3274	0.3274	0.3274	0.3274	0.3274	0.3274	0.3274	0.3274	0.3274	0.3274
C	0	0	0	0	0	0	0	0	0	0	0
ω	5	6	7	8	9	10	11	12	13	14	15
ϕ	0	0	0	0	0	0	0	0	0	0	0
SSR	12.8287	12.8287	12.8287	12.8287	12.8287	12.8287	12.8287	12.8287	12.8287	12.8287	12.8287
Panel B. Optimized parameter values for model 2.											
Specification	1	2	**3**	4	5	6	7	8	9	10	11
A^{**}	10.5677	10.7060	**9.5698**	10.0077	10.3616	10.0828	9.7507	10.2227	10.13027	10.0247	10.0442
B^{**}	−1.7677	−1.8883	**−0.9368**	−1.2911	−1.5903	−1.3553	−1.0805	−1.4687	−1.3924	−1.3043	−1.3199
t_c^{**}	11.2937	11.2993	**11.2183**	11.2490	11.2745	11.2476	11.2296	11.2841	11.2672	11.2572	11.2721
β^{**}	0.2826	0.2713	**0.4085**	0.3414	0.3015	0.3316	0.3778	0.3166	0.3267	0.3394	0.3373
C^{**}	0.0264	−0.0254	**0.0379**	0.0318	−0.0281	0.0310	0.0351	−0.0300	0.0305	0.0316	−0.0315
ω^{**}	15.0000	15.0000	**15.0000**	15.0000	14.9898	14.9672	15.0000	15.0000	15.0000	15.0000	15.0000
ϕ^{**}	−21.1746	−18.0431	**−14.7420**	−14.8028	−11.6909	−8.4508	−8.4803	−5.4487	−2.2749	−2.2527	0.8579
SSR	6.0401	6.0431	**6.0080**	6.0255	6.0360	6.0297	6.0160	6.0314	6.0289	6.0257	6.0262

This table reports the estimated parameter for the optimized log-period power-law singularity model. The estimation procedure is detailed in Section 3. Panel A of Table 2 reports the corresponding input parameters using $\mathbf{\Phi}_1^* = (33.24, \quad -19.45, \quad 152, \quad 0.10)$ from the first estimation step and setting $C = 0$, and $\phi = 0$, while allowing ω to vary across various model specifications with $\in \{5, 6, \ldots, 14, 15\}$. Panel A of Table 2 reports the corresponding input parameters, Panel B of Table 2 reports the optimized parameters using the following constraints $t_c \geq T + 1$, $0.1 \leq \beta \leq 0.9$, and $5 \leq \omega \leq 15$. The sample period is from December 2, 2015 to June 11, 2024 comprising 2147 daily observations. **Bold** figures indicate the model exhibiting the minimum sum of squared residuals (SSR).

Table 3
Descriptive statistics of average parameter estimates for various model calibrations.

	A	B	t_c	β	C	ω	ϕ
Mean	10.1335 * **	−1.3996 * **	11.1285 * **	0.3304 * **	0.0100	14.9961 * **	−9.6821 * **
(t-statistic)	(102.3257)	(−16.8304)	(80.6654)	(27.9103)	(1.0766)	(4937.5960)	(−4.5418)
Median	10.0828	−1.3553	11.2672	0.3316	0.0305	15.0000	−8.4803
Maximum	10.7060	−0.9368	11.2993	0.4085	0.0379	15.0000	0.8579
Minimum	9.5698	−1.8883	9.7507	0.2713	−0.0315	14.9672	−21.1746
Std.Dev.	0.3285	0.2758	0.4576	0.0393	0.0308	0.0101	7.0702
Skewness	0.1271	−0.1974	−2.8329	0.4183	−0.5470	−2.4563	−0.0912
Kurtosis	2.5392	2.5332	9.0554	2.7965	1.3447	7.5297	1.8671
Jarque-Bera	0.1269	0.1713	31.5194	0.3398	1.8043	20.4657	0.6035
(p-value)	(0.9385)	(0.9179)	(0.0000)	(0.8438)	(0.4057)	(0.0000)	(0.7395)

* ** Statistically significant on a 1 % level.
This table reports the descriptive statistics for the average parameter estimates for calibrations reported in Panel B of Table 2. The Jarque-Bera tests and corresponding p-values are also reported. The sample period is from December 2, 2015 to June 11, 2024 comprising 2147 daily observations.

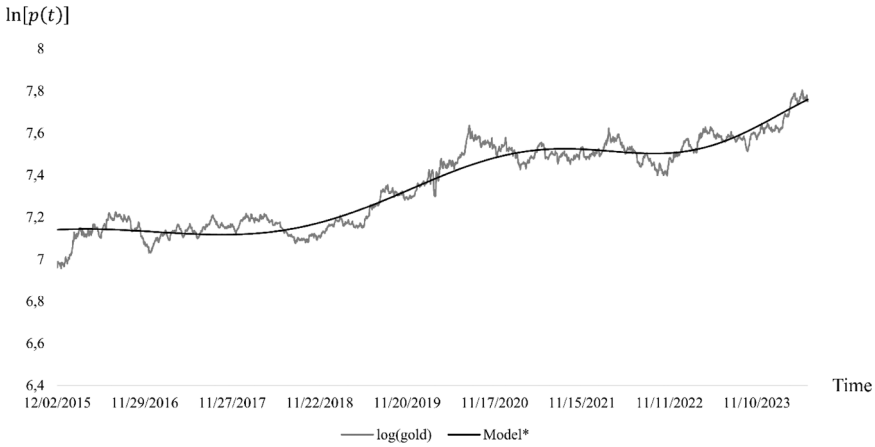

Fig. 2. The log-prices of gold futures and the optimized log-period power-law singularity model for the in-sample period.

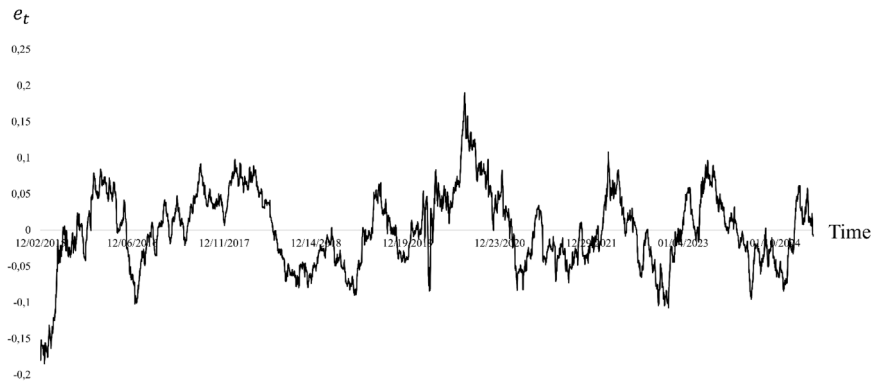

Fig. 3. Residuals of the optimized log-period power-law singularity model.

in-sample period, to calibrate the LPPLS model. Whereas the prediction of the critical time derived from the main analysis is about five years in the future, this robustness check allows us to exclude more than one year of data to calibrate the LPPLS model. Recall from Fig. 5 that the third local peak in the log-prices for gold was reached on August 22, 2011—that is, roughly five years from September 14, 2006.

Table 9 reports the results derived from the model specifications using Eq. (1), whereas Table 10 reports the results derived from the optimized LPPLS model specifications derived from using Eq. (2). From Table 10, we observe that the optimal model 2 specification predicts $t_c^{**} = 9.5038$, which corresponds to March 21, 2007. Because the actual peak of the bubble was reached on August 11, 2011, the LPPLS model predicts the crash 1121 trading days too early. Fig. 8 visualizes the time series evolution of the optimal LPPLS model

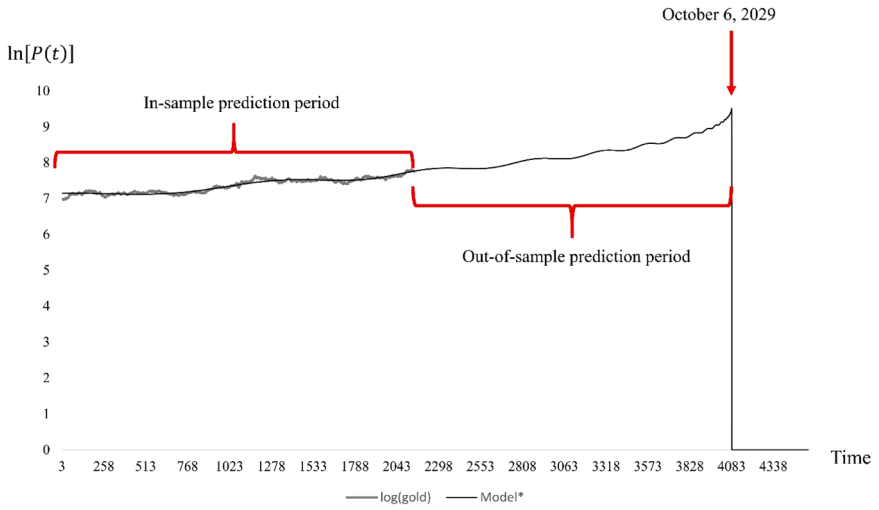

Fig. 4. Predicted evolution of the log-prices for gold futures using the optimized log-period power-law singularity model.

Table 4
Testing the residuals of the log-period power-law singularity model using the 2015—2024 sample.

Model specification	$\widehat{\lambda}$	Critical values	
		5 %	1 %
No deterministic terms ($\delta_0 = \delta_1 = 0$)	−4.7946 ***	−1.94	−2.56
(p-value)	(0.0000)		
Constant ($\delta_1 = 0,\ \delta_1 \neq 0$)	−4.7946 ***	−2.86	−3.43
(p-value)	(0.0001)		
Constant and trend ($\delta_0 \neq 0,\ \delta_1 \neq 0$)	−4.7937 **	−3.41	−3.96
(p-value)	(0.0000)		

* ** Statistically significant on a 1 % level.
This table reports the estimated test statistics for various ADF tests implemented for residuals of the optimized log-periodic power-law singularity model derived from the parameter vector $\mathbf{\Phi}_{2,j}^{**} = \left(A_j^{**},\ B_j^{**},\ t_{c,j}^{**},\ \beta_j^{**}, C_j^{**},\ \omega_j^{**},\ \phi_j^{**}\right)$ with $j = 3$. The critical values for the 5 % and 1 % significance levels, and the p-values. Following Grobys (2023), the Schwarz-Criterion (SC) is used for selection of the optimal lags. As a result, all model specifications employ a lag-order of $p = 0$ as suggested by the SC. The sample period is from December 2, 2015 to June 11, 2024 comprising 2147 daily observations.

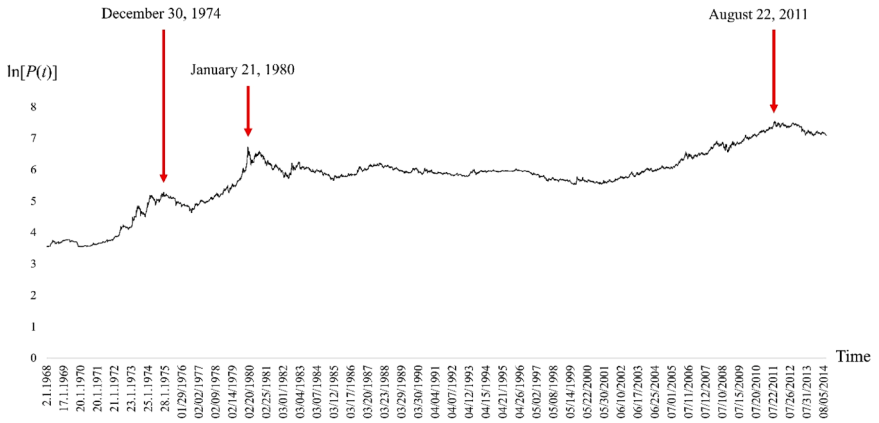

Fig. 5. The evolution of log-prices for gold during the 1968—2014 period.

Table 5
Calibrating the power-law model for logarithmic prices of gold using the 1970—1973 sample.

Panel A. Initial parameter values for model 1.					
Specification	A	B	$\overline{\beta}$	$t_c = T + 1$	SSR
1	4.7207	−1	0.2	4.0240	185.1988
2	4.7207	−1	0.4	4.0240	271.0666
3	4.7207	−1	0.6	4.0240	545.5470
4	4.7207	−1	0.8	4.0240	1135.5740
Panel B. Optimized parameter values for model 1.					
Specification	A^*	B^*	β^*	t_c^*	SSR
1	6.7321	−2.1346	0.2825	4.6799	10.9531
2	**9.8498**	**−5.0884**	**0.1449**	**4.9169**	**10.6763**
3	8.3999	−3.6999	0.1872	4.8473	10.7576
4	7.4261	−2.7806	0.2310	4.7541	10.8481

This table reports the estimated parameter for the plain log-period power-law singularity model. The estimation procedure is detailed in Section 3. Whereas Panel A of Table 5 reports the sum of squared residuals for several initial model specifications, Panel B of Table 5 reports the estimated parameter vector $\mathbf{\Phi}_1^* = (A^*, \quad B^*, \quad t_c^*, \quad \beta^*)$ under the constraints $t_c \geq T + 1$, and $0.1 \leq \beta \leq 0.9$. The sample period used to calibrate the model is from January 16, 1970 to December 31, 1973 comprising 1005 daily observations. **Bold** figures indicate the model exhibiting the minimum sum of squared residuals (SSR).

along with the log-prices for gold, covering a sample from July 19, 1999, to September 30, 2014, whereas Figure A.3 shows the evolution of the residuals derived from the optimal LPPLS model specification covering the in-sample period (i.e., July 19, 1999, to September 14, 2006). In Table A.4. in the Appendix, the results from ADF tests are reported. We observe from Table A.4 that various ADF test statistics suggest that the residuals plotted in Figure A.2 are stationary. Hence, we infer that the optimized LPPLS model indeed produces stationary residuals at a 1 % significance level. Overall, the results suggest that the LPPLS model is also capable of (a) detecting bubble formation in the 2000s, as indicated by the statistically significant LPPLS signature, but (b) it failed to predict the critical time.

5. Discussion

5.1. How do our results align with earlier literature?

The main results indicate that gold futures show strong evidence for an ongoing bubble formation in the ex-post GFC period, eventually reaching a critical time in October 2029. Evidence for bubble formation in the prices for gold is in line with Pindyck (1993), Bertus and Stanhouse (2001), and Went et al. (2009), who documented that gold is subject to reoccurring bubble formations. Whereas the majority of those studies made use of CY to explore bubble formations, as stressed by O'Connor et al., (2015), the present study follows Johansen and Sornette (1999), Sornette (2017), and Grobys (2023), among others, in employing the LPPLS model, which is known to deliver outstanding performance to detect financial bubble formations (Shu and Zhu, 2020). Various optimized LPPLS model specifications of our main analysis suggest that the predicted critical time varies between October 6, 2029, and November 5, 2029. Compared with other LPPLS model predictions, this time interval is surprisingly narrow. For example, the well-known stock market crash of October 19, 1987, where the Dow Jones 30 index dropped by more than 20 %, has been subject to intense investigations (Sornette, 2017). Using the LPPLS model and a calibrating sample ranging between January 2, 1980, and December 31, 1986, comprising 1770 daily observations, Grobys (2023) found that the predicted critical time derived from the optimized LPPLS model varies between $t_c^{**} = 8.25$ (viz., February 29, 1988) and $t_c^{**} = 10.53$ (viz., May 30, 1990), whereas the optimal LPPLS model suggests $t_c^{**} = 8.26$, which corresponds to March 1, 1988.

That is, whereas the optimal LPPLS model in Grobys' (2023) study predicts the critical time 92 days too late, the results derived from other optimized LPPLS models suggest a range of the critical time t_c^{**} corresponding to 571 days (viz., between February 29, 1988, and May 30, 1990)—exceeding the range derived from optimized LPPLS models by a substantial margin. Similar evidence to what was in Grobys' (2023) study was documented in Sornette (2017). However, Sornette (2017) clarified that the LPPLS model typically predicts the critical time "systematically later than the real time of the crash: the critical time t_c is included in the log-periodic power law structure of the bubble, whereas the crash is randomly triggered with a biased probability increasing strongly close to t_c" (p. 332).

Furthermore, the results derived from our robustness checks show that the LPPLS model is capable of (a) identifying the gold bubble formations in the 1970s, 1980s, and early 2000s and (b) predicting at least two of them (i.e., the bubble formations in the 1970s and 1980s) with a high level of accuracy. Specifically, for back-testing the LPPLS model for the bubble formations in the 1970s and 1980s, we follow the mainstream literature on empirically testing the LPPLS model by excluding the last year of observations before the bubble formations reached their peaks. Our calibrated models provide evidence that the optimal LPPLS model predicts the bubble peaks either 47 trading days too late or 63 trading days too early, corresponding to an average error of $\frac{-47+63}{2} = 8$ days. Surprisingly, the evidence suggests that LPPLS model calibrations appear to predict the peaks for gold bubble formations with a considerably higher level of accuracy than when applied to predict bubble peaks in equity markets. For example, Grobys (2023) argued that his optimal LPPLS model, which he used to predict the US stock market crash that occurred on October 23, 1929, showed an average of 181 days,

Table 6
Optimizing the log-period power-law singularity model for logarithmic prices of gold futures using the 1970—1973 sample.

Panel A. Initial parameter values for model 2.											
Specification	1	2	3	4	5	6	7	8	9	10	11
A^*	9.8498	9.8498	9.8498	9.8498	9.8498	9.8498	9.8498	9.8498	9.8498	9.8498	9.8498
B^*	−5.0884	−5.0884	−5.0884	−5.0884	−5.0884	−5.0884	−5.0884	−5.0884	−5.0884	−5.0884	−5.0884
t_c^*	4.9169	4.9169	4.9169	4.9169	4.9169	4.9169	4.9169	4.9169	4.9169	4.9169	4.9169
β^*	0.1449	0.1449	0.1449	0.1449	0.1449	0.1449	0.1449	0.1449	0.1449	0.1449	0.1449
C	0	0	0	0	0	0	0	0	0	0	0
ω	5	6	7	8	9	10	11	12	13	14	15
ϕ	0	0	0	0	0	0	0	0	0	0	0
SSR	10.6764	10.6764	10.6764	10.6764	10.6764	10.6764	10.6764	10.6764	10.6764	10.6764	10.6764
Panel B. Optimized parameter values for model 2.											
Specification	1	2	**3**	4	5	6	7	8	9	10	11
A^{**}	9.4873	9.6012	**5.4160**	13.3485	13.3589	13.3566	13.3485	13.3599	13.3624	13.3176	13.3712
B^{**}	−4.5264	−4.6379	**−0.6266**	−8.4595	−8.4679	−8.4664	−8.4591	−8.4681	−8.4710	−8.4345	−8.4781
t_c^{**}	5.3935	5.3976	**5.2213**	5.0390	5.0420	5.0402	5.0398	5.0427	5.0418	5.0301	5.0445
β^{**}	0.1651	0.1617	**0.7178**	0.1000	0.1000	0.1000	0.1000	0.1000	0.1000	0.1000	0.1000
C^{**}	0.0242	0.0237	**0.1002**	−0.0101	0.0101	0.0101	0.0101	0.0101	−0.0101	−0.0101	−0.0101
ω^{**}	5	5	**5**	11.4613	11.4728	11.4644	11.4655	11.4808	11.4730	11.4103	11.4909
ϕ^{**}	−0.1751	−0.1852	**0.5546**	−4.6891	−1.5750	−1.5564	−1.5563	−1.5849	1.5685	1.6884	1.5384
SSR	5.8903	5.8907	**5.8302**	6.3898	6.3897	6.3897	6.3898	6.3897	6.3896	6.3907	6.3895

This table reports the estimated parameter for the optimized log-period power-law singularity model. The estimation procedure is detailed in Section 3. Panel A of Table 6 reports the corresponding input parameters using $\mathbf{\Phi}_1^*$ from the first estimation step and setting $C = 0$, and $\phi = 0$, while allowing ω to vary across various model specifications with $\in \{5,\ 6, \ldots, 14,\ 15\}$. Panel B of Table 6 reports the optimized parameters using the following constraints $t_c \geq T + 1$, $0.1 \leq \beta \leq 0.9$, and $5 \leq \omega \leq 15$. The sample period used to optimize the model is from January 16, 1970 to December 31, 1973 comprising 1005 daily observations. **Bold** figures indicate the model exhibiting the minimum sum of squared residuals (SSR).

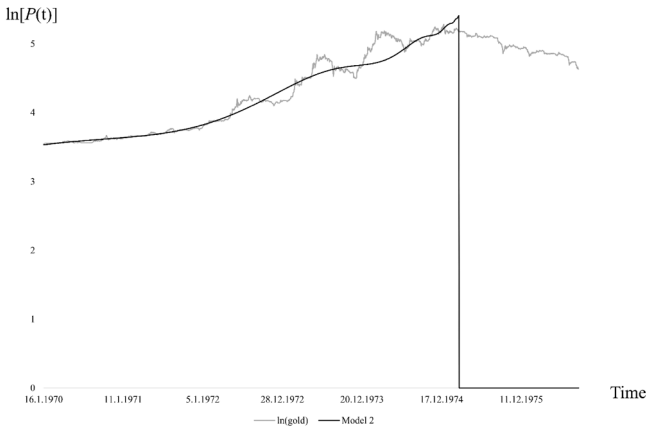

Fig. 6. Predicted evolution of the log-prices for gold during the bubble formation in the 1970s using the optimized log-period power-law singularity model.

Table 7
Calibrating the power-law model for logarithmic prices of gold using the 1976—1979 sample.

Panel A. Initial parameter values for model 1.					
Specification	A	B	$\overline{\beta}$	$t_c = T + 1$	SSR
1	5.5318	−1	0.2	2.4920	213.5490
2	5.5318	−1	0.4	2.4920	241.5790
3	5.5318	−1	0.6	2.4920	310.1090
4	5.5318	−1	0.8	2.4920	424.0890
Panel B. Optimized parameter values for model 1.					
Specification	A^*	B^*	β^*	t_c^*	SSR
1	7.6508	−1.5625	0.3814	4.8623	1.5780
2	6.2299	−0.5841	0.6522	3.9869	1.5691
3	5.9347	−0.5019	0.6761	3.3606	1.5710
4	**5.8863**	**−0.4541**	**0.7254**	**3.3697**	**1.5669**

This table reports the estimated parameter for the plain log-period power-law singularity model. The estimation procedure is detailed in Section 3. Whereas Panel A of Table 7 reports the sum of squared residuals for several initial model specifications, Panel B of Table 7 reports the estimated parameter vector $\mathbf{\Phi}_1^* = (A^*, \quad B^*, \quad t_c^*, \quad \beta^*)$ under the constraints $t_c \geq T + 1$, and $0.1 \leq \beta \leq 0.9$. The sample period used to calibrate the model is August 30, 1976 to January 21, 1979 comprising 622 daily observations. **Bold** figures indicate the model exhibiting the minimum sum of squared residuals (SSR).

whereas Sornette (2017) documented that his proposed LPPLS model calibration produced two optimums: 30.52 and 30.35, resulting in an average error of 228 days.[8] Grobys (2023) and Sornette (2017) documented similar evidence for the performance of various LPPLS models used to predict other stock market crashes. Overall, the LPPLS model appears to do a better job when used to predict bubble formations in the gold market.

On the other hand, the main analysis predicts that the current bubble formation in the market for gold will reach its peak in about ≈ 5 years in the future. Because the in-sample time window used to calibrate the LPPLS model is $T = 2147$ days, corresponding to approximately ≈ 8.59 years, the predicted time of the crash is still in the less distant future than twice the calibration period, that is, $t_c^* < 2T$. Hence, we do not need to impose the additional constraint $t_c^* < 2T$ in the optimization procedure (Sornette, 2017). Hence, to test whether the LPPLS model can predict critical times in the distant future (viz., $t_c^* > 250$), we have attempted to predict the bubble peak that occurred in the prices for gold on August 22, 2011, by excluding 1250 days—that is, the sample period from September 14, 2006, to August 22, 2011—from the in-sample time window used to calibrate the LPPLS model. Calibrating the LPPLS over the sample from July 19, 1999, to September 14, 2006, comprising 1745 daily observations, the model (a) identifies a statistically significant bubble in terms of a LPPLS signature, and (b) the model predicts that the bubble would reach its peak on March 21, 2007. Self-evidently, historical evidence clearly suggests that a regime switch in gold prices did not occur during the GFC period. A potential explanation for the inability of the LPPLS model to predict that a crash could be a manifestation of the spillover effect originating from

[8] Note that the LPPLS models used in Grobys (2023) and Sornette (2017) that are referred to here use LPPLS model calibrations, where the last year of observations before reaching the bubble peaks were excluded. By this, we ensure that the results are comparable because Sornette highlighted that the predictions for the critical time t_c, derived from LPPLS model calibrations, are increasingly precise as we approach the critical time: "Approximately a year before the crash, the fit begins to lock in on the date of the crash with increasing precision" (2017, p. 330).

Table 8
Optimizing the log-period power-law singularity model for logarithmic prices of gold futures using the 1976—1979 sample.

Panel A. Initial parameter values for model 2.											
Specification	1	2	3	4	5	6	7	8	9	10	11
A^{*}	5.8863	5.8863	5.8863	5.8863	5.8863	5.8863	5.8863	5.8863	5.8863	5.8863	5.8863
B^{*}	−0.4541	−0.4541	−0.4541	−0.4541	−0.4541	−0.4541	−0.4541	−0.4541	−0.4541	−0.4541	−0.4541
t_c^{*}	3.3697	3.3697	3.3697	3.3697	3.3697	3.3697	3.3697	3.3697	3.3697	3.3697	3.3697
β^{*}	0.7254	0.7254	0.7254	0.7254	0.7254	0.7254	0.7254	0.7254	0.7254	0.7254	0.7254
C	0	0	0	0	0	0	0	0	0	0	0
ω	5	6	7	8	9	10	11	12	13	14	15
ϕ	0	0	0	0	0	0	0	0	0	0	0
SSR	1.5669	1.5669	1.5669	1.5669	1.5669	1.5669	1.5669	1.5669	1.5669	1.5669	1.5669
Panel B. Optimized parameter values for model 2.											
Specification	1	2	3	4	5	6	7	8	**9**	**10**	**11**
A^{**}	5.5702	5.5043	5.5042	5.5043	5.5041	5.4812	5.5041	5.4816	**5.8515**	**5.8506**	**5.8521**
B^{**}	−0.2106	−0.2769	−0.2769	−0.2770	−0.2768	−0.0040	−0.2768	−0.0039	**−0.4581**	**−0.4574**	**−0.4587**
t_c^{**}	3.1360	2.6694	2.6695	2.6694	2.6695	4.0916	2.6694	4.0997	**3.2459**	**3.2456**	**3.2460**
β^{**}	1.2359	1.0725	1.0727	1.0722	1.0731	4.3303	1.0731	4.3562	**0.7173**	**0.7180**	**0.7167**
C^{**}	−0.0877	−0.1025	−0.1025	0.1024	0.1026	0.5587	0.1026	−0.5620	**−0.0663**	**0.0664**	**0.0662**
ω^{**}	6.567256	5	5	5.0000	5.0000	5.0000	5.0000	5.0000	**15.0000**	**15.0000**	**15.0000**
ϕ^{**}	−0.1140	2.5374	2.5367	5.6790	5.6781	2.4931	5.6787	5.6241	**−2.5013**	**0.6428**	**0.6401**
SSR	1.3781	1.3360	1.3360	1.3360	1.3360	1.2291	1.3360	1.2285	**0.8250**	**0.8250**	**0.8250**

This table reports the estimated parameter for the optimized log-period power-law singularity model. The estimation procedure is detailed in Section 3. Panel A of Table 8 reports the corresponding input parameters using $\mathbf{\Phi}_1^{*}$ from the first estimation step and setting $C = 0$, and $\phi = 0$, while allowing ω to vary across various model specifications with $\in \{5,\ 6, \ldots, 14,\ 15\}$. Panel B of Table 8 reports the optimized parameters using the following constraints $t_c \geq T + 1$, $0.1 \leq \beta \leq 0.9$, and $5 \leq \omega \leq 15$. The sample period used to optimize the model is from August 30, 1976 to January 21, 1979 comprising 622 daily observations. **Bold** figures indicate the model exhibiting the minimum sum of squared residuals (SSR).

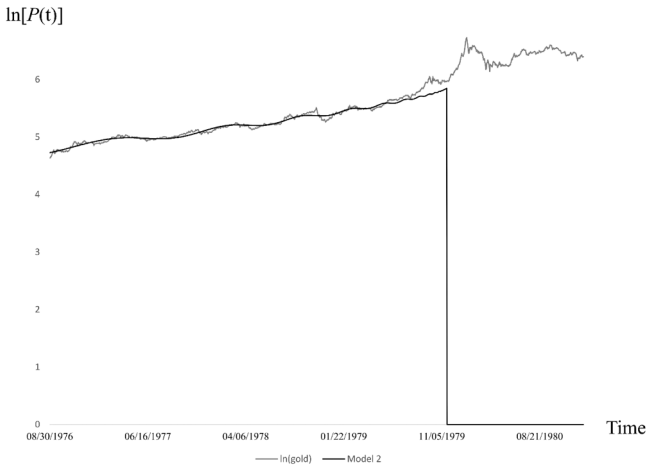

Fig. 7. Predicted evolution of the log-prices for gold during the bubble formation in the 1980s using the optimized log-period power-law singularity model.

Table 9
Calibrating the power-law model for logarithmic prices of gold using the 1999—2006 sample.

Panel A. Initial parameter values for model 1.					
Specification	A	B	$\overline{\beta}$	$t_c = T + 1$	SSR
1	6.3733	−1	0.2	6.9840	968.8183
2	6.3733	−1	0.4	6.9840	2073.3020
3	6.3733	−1	0.6	6.9840	4591.2530
4	6.3733	−1	0.8	6.9840	9995.3180
Panel B. Optimized parameter values for model 1.					
Specification	A^*	B^*	β^*	t_c^*	SSR
1	**7.4426**	**−1.1784**	**0.2344**	**7.3066**	**7.0211**
2	7.1510	−0.9133	0.2800	7.2160	7.0703
3	7.2977	−1.0471	0.2543	7.2610	7.0413
4	7.2145	−0.9708	0.2684	7.2370	7.0564

This table reports the estimated parameter for the plain log-period power-law singularity model. The estimation procedure is detailed in Section 3. Whereas Panel A of Table 9 reports the sum of squared residuals for several initial model specifications, Panel B of Table 9 reports the estimated parameter vector $\mathbf{\Phi}_1^* = (A^*, \quad B^*, \quad t_c^*, \quad \beta^*)$ under the constraints $t_c \geq T + 1$, and $0.1 \leq \beta \leq 0.9$. The sample used to calibrate the model is July 19, 1999 to September 14, 2006 comprising 1745 daily observations. **Bold** figures indicate the model exhibiting the minimum sum of squared residuals (SSR).

the bubble formation in the housing market.

Similar evidence was documented by Grobys' (2023), who attempted to predict the US stock market crash of October 15, 2008. Using a sample of daily data on the S&P 500 covering the period October 9, 2002, to December 31, 2007 to calibrate the LPPLS model, Grobys' (2023) results suggested (a) evidence for a statistically significant LPPLS signature and (b) the arrival of a finite-time singularity on August 19, 2011. The LPPLS model is designed to model endogenous behavior manifested in internal bubble mechanisms with positive (negative) feedback mechanisms. As pointed out by Bianco (2008), early signs of the subprime mortgage crisis, popularly known as the "mortgage meltdown," came to the public's attention in the wake of a steep rise in home foreclosures in 2006. Market participators observing this issue might have allocated their funds to gold and, as a result, pushed the prices for gold even further, hence impeding the gold bubble from bursting in 2007. Therefore, the fact that the LPPLS model calibration produces a "false positive" for March 21, 2007, could be a manifestation of an external event that interfered with the endogenous mechanisms at play in the market for gold. Future research is encouraged to explore this issue in more detail.

5.2. Implications

Because gold is often referred to as a safe haven asset, a question that inevitably arises is whether gold is a sustainable safe haven. Baur and McDermott (2010) concluded that gold served as a strong safe haven for most developed markets during the peak of the GFC. Lucey and Li (2014) found that gold has exhibited periods when it did not act as either a safe haven or a hedge for US stocks and bonds. Similarly, using a data-driven approach by adopting a Markov switching model to examine whether gold is a safe haven, He et al. (2018) concluded that gold consistently serves as a hedge, but no distinct safe haven state exists between gold and UK or US stock

Table 10
Optimizing the log-period power-law singularity model for logarithmic prices of gold futures using the 1999—2006 sample.

Panel A. Initial parameter values for model 2.											
Specification	1	2	3	4	5	6	7	8	9	10	11
A^{*}	7.4426	7.4426	7.4426	7.4426	7.4426	7.4426	7.4426	7.4426	7.4426	7.4426	7.4426
B^{*}	−1.1784	−1.1784	−1.1784	−1.1784	−1.1784	−1.1784	−1.1784	−1.1784	−1.1784	−1.1784	−1.1784
t_c^{*}	7.3066	7.3066	7.3066	7.3066	7.3066	7.3066	7.3066	7.3066	7.3066	7.3066	7.3066
β^{*}	0.2344	0.2344	0.2344	0.2344	0.2344	0.2344	0.2344	0.2344	0.2344	0.2344	0.2344
C	0	0	0	0	0	0	0	0	0	0	0
ω	5	6	7	8	9	10	11	12	13	14	15
ϕ	0	0	0	0	0	0	0	0	0	0	0
SSR	7.0211	7.0211	7.0211	7.0211	7.0211	7.0211	7.0211	7.0211	7.0211	7.0211	7.0211
Panel B. Optimized parameter values for model 2.											
Specification	1	2	3	4	5	6	7	8	9	10	11
A^{**}	9.2522	9.4976	**9.5038**	9.0062	8.2556	8.3801	7.8496	7.8622	7.5783	7.6116	6.9206
B^{**}	−2.9780	−3.1816	**−3.1867**	−2.7363	−1.9897	−2.1132	−1.5874	−1.5998	−1.2697	−1.3015	−0.6931
t_c^{**}	7.3643	7.4996	**7.5040**	7.3489	7.3369	7.3398	7.3262	7.3261	7.4506	7.4548	7.1629
β^{**}	0.1000	0.1000	**0.1000**	0.1074	0.1426	0.1353	0.1732	0.1721	0.2329	0.2285	0.3482
C^{**}	−0.0229	−0.0210	**0.0209**	0.0247	−0.0323	−0.0308	0.0388	0.0385	−0.0245	0.0240	0.0437
ω^{**}	5.047689	5.430097	**5.442517**	5.0006	5.0000	5.0000	5.0007	5.0000	14.9684	15.0000	14.8045
ϕ^{**}	1.1095	0.3805	**3.4969**	4.3492	7.5315	7.5225	10.7066	10.7082	−4.2049	−1.1319	0.0151
SSR	3.0851	3.0471	**3.0469**	3.1049	3.1648	3.1504	3.2350	3.2323	5.4905	5.4901	5.2397

This table reports the estimated parameter for the optimized log-period power-law singularity model. The estimation procedure is detailed in Section 3. Panel A of Table 10 reports the corresponding input parameters using $\mathbf{\Phi}_1^{*}$ from the first estimation step and setting $C = 0$, and $\phi = 0$, while allowing ω to vary across various model specifications with $\in \{5, 6, \ldots, 14, 15\}$. Panel B of Table 10 reports the optimized parameters using the following constraints $t_c \geq T + 1$, $0.1 \leq \beta \leq 0.9$, and $5 \leq \omega \leq 15$. The sample period used to optimize the model is from July 19, 1999 to September 14, 2006 comprising 1745 daily observations. **Bold** figures indicate the model exhibiting the minimum sum of squared residuals (SSR).

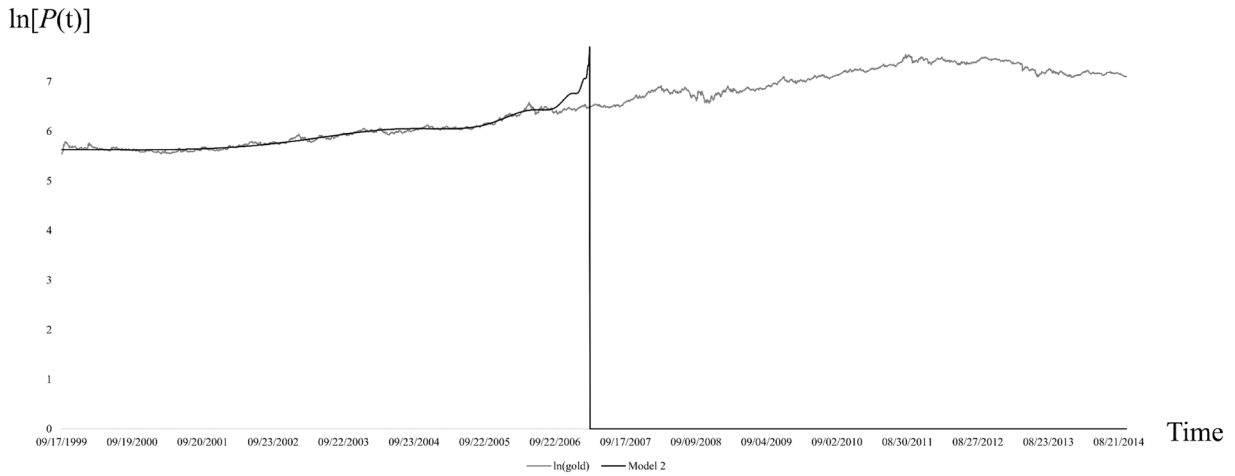

Fig. 8. Predicted evolution of the log-prices for gold during the bubble formation in the early 2000s using the optimized log-period power-law singularity model.

markets. Adding to this literature, the present study argues that, from an investor's perspective, the absence of correlation may be irrelevant if a "safe haven asset" is subject to reoccurring crashes itself. Therefore, sustainability should be a precondition that a safe haven asset needs to fulfill. Because the present study provides strong evidence for reoccurring bubble formations in the prices for gold that, historically, resulted in severe corrections, we are forced to conclude that gold does not qualify as a safe haven candidate. Investors wishing to employ gold for either hedging purposes or as a safe haven asset to optimize the risk of their asset portfolios are advised to take caution.

5.3. Limitations

The present study has, of course, its limitations. For instance, a general concern regarding the application of the LPPLS model could be that, in general, model parameters should be static and should not significantly change as additional data arrive. In this regard, Brée et al. (2013) stressed that the critical times derived from LPPS model calibrations fluctuate by a substantial margin as the time series input data change. This, however, should not come as a great surprise as Sornette (2017) highlighted that the predictions for the critical times derived from LPPLS model calibrations are systematically biased because the crash is systematically predicted "later than the real time of the crash: the critical time t_c is included in the log-periodic power law structure of the bubble, whereas the crash is randomly triggered with a biased probability increasing strongly close to t_c " (p. 332). Furthermore, Sornette (2017) argued that the predictions for the critical time t_c, derived from LPPLS model calibrations are increasingly precise as we approach the critical time: "Approximately a year before the crash, the fit begins to lock in on the date of the crash with increasing precision" (p. 330).

Some features of the LPPLS model calibrations documented in the present study are also noteworthy. First, the estimated critical time—depending on the calibrated model—ranges between October 6, 2029, and November 5, 2029, which is a very narrow interval with respect to the fact that the arrival of the finite-time singularity is expected to take place about five years in the future. Second, other studies (e.g., Grobys, 2023; Sornette, 2017) were forced to impose further model constraints, ensuring that the estimated critical time did not exceed twice that of the sample length (e.g., $t_c^* < 2T$). However, in the present study, imposing this additional restriction was *not* necessary because the arrival of the finite-time singularity is expected for $t_c^* < 2T$. Nonetheless, as more data arrive, future studies are encouraged to re-examine our model estimations.

6. Conclusion

Bubble formations of financial assets are a typical manifestation of speculation. In this regard, it is noteworthy that the LPPLS model has a strong theoretical foundation incorporating imitation among traders, which manifests in herding behavior. Whereas the literature on bubble formations in the market for gold is still in its infancy, the current study adopts the LPPLS model to explore the potential arrival of a finite-time singularity in the log-prices of gold futures. The literature on investigating gold as a financial asset documents that the dynamics constituting the supply-and-demand relationship in the market for gold has undergone some substantial changes since the early 2000s. In particular, the GFC might have triggered an unprecedented demand for gold. Is gold in the process of an ongoing bubble formation?

This is the first study examining whether gold is forming a bubble in the ex-post GFC period. Identifying a local trough in the prices of gold on December 2, 2015, we calibrate the LPPLS model using an in-sample time window ranging from December 2, 2015, to June 11, 2024, comprising 2147 daily observations. The main results are that (a) the prices for gold manifest a strong LPPLS signature signaling faster-than-exponential growth that is not sustainable, (b) the optimal calibrated model predicts the arrival of a finite-time singularity (viz., critical time) on October 6, 2029, and (c) the critical times predicted by other optimized LPPLS models suggest a

surprisingly narrow time window for the occurrence of the regime switch (i.e., between October 6, 2029, and November 5, 2029).

Our study opens various interesting avenues for future research. For example, the robustness checks of the present research provide ample evidence that the LPPLS model appears to do a better job when used to predict price bubble formations in the market for gold as opposed to equity markets. Future research is encouraged to explore this issue in more detail. Moreover, evidence for "false positives" produced by LPPLS calibrations—manifested here in identifying a significant bubble formation in 1999–2006 that, for some reason, did not result in the predicted regime switch—needs further investigation. Because various studies have documented false positives produced by LPPLS model calibrations (e.g., Brée et al., 2013; Grobys, 2023), the following question arises: What are the root causes for this issue? The present study argues that a commonality among recently documented false positives could be that external mechanisms (e.g., GFC) that had severe economic consequences could have disturbed the endogenous mechanism modeled by the LPPLS model. Future research is still needed to clarify this issue.

Author statement

The author conducted the study by himself.
The author has no relevant financial or non-financial interests to disclose.
The author declares that no funds, grants, or other support were received during the preparation of this manuscript.

CRediT authorship contribution statement

Klaus Grobys: Writing – review & editing, Writing – original draft, Visualization, Validation, Supervision, Software, Resources, Project administration, Methodology, Investigation, Formal analysis, Data curation, Conceptualization.

Appendix

Table A.1. Descriptive statistics for the log-returns of gold futures

Metric	log-returns of gold futures
Mean	0.0365
Median	0.0468
Maximum	8.5890
Minimum	−9.8105
Std. Dev.	1.0948
Skewness	−0.3182
Kurtosis	8.1870
Jarque-Bera	6711.3620
(*p*-value)	(0.0000)
Observations	5898

This table reports the descriptive statistics for the daily log-returns of gold futures. The Jarque-Bera test and the corresponding *p*-value is also reported. The sample period is from December 2, 2015 to June 11, 2024.

Table A.2. Testing the residuals of the optimized log-period power-law singularity model using the 1970—1973 sample

Model specification	$\widehat{\lambda}$	Critical values	
		5 %	1 %
No deterministic terms ($\delta_0 = \delta_1 = 0$)	−2.8589 * **	−1.94	−2.56
(*p*-value)	(0.0042)		
Constant ($\delta_1 = 0,\ \delta_1 \neq 0$)	−2.8574 *	−2.86	−3.43
(*p*-value)	(0.0509)		
Constant and trend ($\delta_0 \neq 0,\ \delta_1 \neq 0$)	−2.856	−3.41	−3.96
(*p*-value)	(0.1776)		

This table reports the estimated test statistics for various ADF tests implemented for residuals of the optimized log-periodic power-law singularity model derived from the parameter vector $\mathbf{\Phi}_{2j}^{**} = \left(A_j^{**},\ B_j^{**},\ t_{cj}^{**},\ \beta_j^{**}, C_j^{**},\ \omega_j^{**},\ \phi_j^{**}\right)$ with $j = 3$. The critical values for the 5 % and 1 % significance levels, and the *p*-values. Following Grobys (2023), the Schwarz-Criterion (SC) is used for selection of the optimal lags. As a result, all model specifications employ a lag-order of $p = 0$ as suggested by the SC. The sample period used to optimize the model is from January 16, 1970 to December 31, 1973 comprising 1005 daily observations.
* ** Statistically significant on a 1 % level, * Statistically significant on a 10 % level.

Table A.3. Testing the residuals of the optimized log-period power-law singularity model using the 1976—1979 sample

Model specification	$\widehat{\lambda}$	Critical values	
		5 %	1 %
No deterministic terms ($\delta_0 = \delta_1 = 0$)	−4.9874 ***	−1.94	−2.56
(p-value)	(0.0000)		
Constant ($\delta_1 = 0,\ \delta_1 \neq 0$)	−4.9831 ***	−2.86	−3.43
(p-value)	(0.0000)		
Constant and trend ($\delta_0 \neq 0,\ \delta_1 \neq 0$)	−4.9789 ***	−3.41	−3.96
(p-value)	(0.0002)		

This table reports the estimated test statistics for various ADF tests implemented for residuals of the optimized log-periodic power-law singularity model derived from the parameter vector $\mathbf{\Phi}_{2j}^{**} = \left(A_j^{**},\ B_j^{**},\ t_{cj}^{**},\ \beta_j^{**}, C_j^{**},\ \omega_j^{**},\ \phi_j^{**}\right)$ with $j = 9$. The critical values for the 5 % and 1 % significance levels, and the p-values. Following Grobys (2023), the Schwarz-Criterion (SC) is used for selection of the optimal lags. As a result, all model specifications employ a lag-order of $p = 0$ as suggested by the SC. The sample period used to optimize the model is from August 30, 1976 to January 21, 1979 comprising 622 daily observations.
* ** Statistically significant on a 1 % level.

Table A.4. Testing the residuals of the optimized log-period power-law singularity model using the 1999—2006 sample

Model specification	$\widehat{\lambda}$	Critical values	
		5 %	1 %
No deterministic terms ($\delta_0 = \delta_1 = 0$)	−5.4432 ***	−1.94	−2.56
(p-value)	(0.0000)		
Constant ($\delta_1 = 0,\ \delta_1 \neq 0$)	−5.4447 ***	−2.86	−3.43
(p-value)	(0.0000)		
Constant and trend ($\delta_0 \neq 0,\ \delta_1 \neq 0$)	−5.4840 ***	−3.41	−3.96
(p-value)	(0.0000)		

This table reports the estimated test statistics for various ADF tests implemented for residuals of the optimized log-periodic power-law singularity model derived from the parameter vector $\mathbf{\Phi}_{2j}^{**} = \left(A_j^{**},\ B_j^{**},\ t_{cj}^{**},\ \beta_j^{**}, C_j^{**},\ \omega_j^{**},\ \phi_j^{**}\right)$ with $j = 3$. The critical values for the 5 % and 1 % significance levels, and the p-values. Following Grobys (2023), the Schwarz-Criterion (SC) is used for selection of the optimal lags. As a result, all model specifications employ a lag-order of $p = 0$ as suggested by the SC. The sample period used to optimize the model is from July 19, 1999 to September 14, 2006 comprising 1745 daily observations.
* ** Statistically significant on a 1 % level.

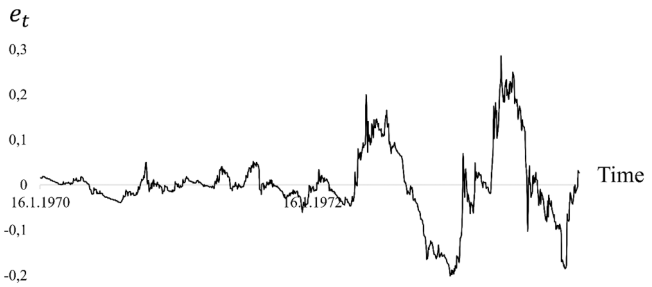

Figure A.1. Residuals of the optimized log-period power-law singularity model used to predict the burst of the gold bubble formation in the 1970s.

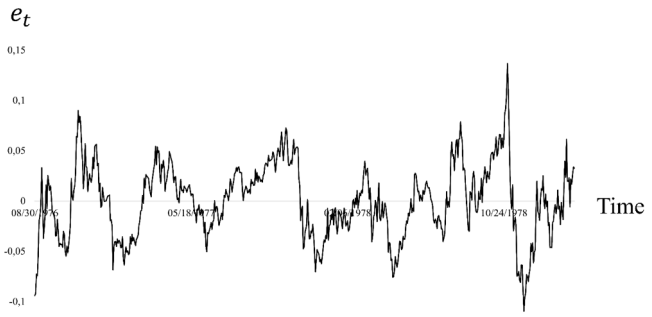

Figure A.2. Residuals of the optimized log-period power-law singularity model used to predict the burst of the gold bubble formation in the 1980s.

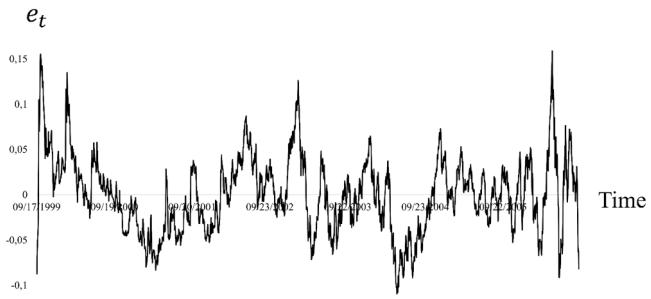

Figure A.3. Residuals of the optimized log-period power-law singularity model used to predict the burst of the gold bubble formation in the early 2000s.

Data availability

Data are online available for free.

References

Baur, D.G., 2013. Exchange-traded funds on gold – A free lunch. FIRN Work. Pap., Univ. West. Aust.
Baur, D.G., McDermott, T.K., 2010. Is gold a safe haven? International evidence. J. Bank. Financ. 34 (8), 1886–1898.
Bertus, M., Stanhouse, B., 2001. Rationale speculative bubbles in the gold futures market: an application of dynamic factor analysis. J. Futures Mark. 21 (1), 79–108.
Bianco, K.M., 2008. The subprime lending crisis: Causes and effects of the mortgage meltdown. CCH, Wolters Kluwer Law & Business, pp. 1–21.
Brée, D.S., Challet, D., Peirano, P.P., 2013. Prediction accuracy and sloppiness of log-periodic functions. Quant. Financ. 13 (2), 275–280.
Grobys, K., 2023. A finite-time singularity in the dynamics of the US equity market: will the US equity market eventually collapse? Int. Rev. Financ. Anal. 89, 102787.
Grobys, K., 2024. No reward—no effort: will Bitcoin collapse near to the year 2140? Financ. Res. Lett. 63, 105294.
He, Z., O'Connor, F., Thijssen, J., 2018. Is gold a sometimes safe haven or an always hedge for equity investors? A Markov-switching CAPM approach for US and UK stock indices. Int. Rev. Financ. Anal. 60, 30–37.
Johansen, A., Sornette, D., 1999. Financial "anti-bubbles": log-periodicity in gold and Nikkei collapses. Int. J. Mod. Phys. C. 10 (4), 563–575.
Johansen, A., Sornette, D., 2001. Finite-time singularity in the dynamics of the world population, economic and financial indices. Phys. A Stat. Mech. Its Appl. 294, 465–502.
Lin, L., Ren, R.E., Sornette, D., 2014. The volatility-confined LPPL model: a consistent model of 'explosive' financial bubbles with mean-reverting residuals. Int. Rev. Financ. Anal. 33, 210–225.
Lucey, B.M., Li, S., 2014. What precious metals act as safe havens, and when? Some US evidence. Appl. Econ. Lett. 22, 35–45.
O'Connor, F.A., Lucey, B.M., Batten, J.A., Baur, D.G., 2015. The financial economics of gold—A survey. Int. Rev. Financ. Anal. 41, 186–205.
Pindyck, R.S., 1993. The present value model of rational commodity pricing. Econ. J. 103, 511–530.
Shu, M., Zhu, W., 2020. Detection of Chinese stock market bubbles with LPPLS confidence indicator. Phys. A Stat. Mech. Its Appl. 557, 124892.
Sornette, D., 2017. Why stock markets crash: Critical events in complex financial systems. Princeton University Press.
Taleb, N.N., 2020. Statistical consequences of fat tails: Real world preasymptotics, epistemology, and applications. STEM Academic Press.
Went, P., Jirasakuldech, B., & Emekter, R. (2009). Bubbles in Commodities.
Wheatley, S., Sornette, D., Huber, T., Reppen, M., Gantner, R.N., 2019. Are bitcoin bubbles predictable? Combining a generalized Metcalfe's Law and the log-periodic power law singularity model. R. Soc. Open Sci. 6 (6), 180538.
Zhang, Q., Sornette, D., Balcilar, M., Gupta, R., Ozdemir, Z.A., Yetkiner, H., 2016. LPPLS bubble indicators over two centuries of the S&P 500 index. Phys. A Stat. Mech. Its Appl. 458, 126–139.
Zhou, W.-X., Sornette, D., 2006. Is there a real estate bubble in the US? Phys. A: Stat. Mech. Its Appl. 361 (1), 297–308.
Zhou, W.-X., Sornette, D., 2009. A case study of speculative financial bubbles in the South African stock market 2003–2006. Phys. A Stat. Mech. Its Appl. 388, 869–880.